10-13-2013

Zebrafish Cytosolic Carboxypeptidases 1 and 5 Are Essential for Embryonic Development

Peter J. Lyons
Andrews University, lyons@andrews.edu

Matthew R. Sapio

Lloyd D. Fricker

THE JOURNAL OF BIOLOGICAL CHEMISTRY VOL. 288, NO. 42, pp. 30454–30462, October 18, 2013

Zebrafish Cytosolic Carboxypeptidases 1 and 5 Are Essential for Embryonic Development*[S]

Received for publication, July 1, 2013, and in revised form, August 30, 2013 Published, JBC Papers in Press, September 10, 2013, DOI 10.1074/jbc.M113.497933

Peter J. Lyons[‡1,2], **Matthew R. Sapio**[§1], **and Lloyd D. Fricker**[‡3]

From the Departments of [‡]*Molecular Pharmacology and* [§]*Neuroscience, Albert Einstein College of Medicine, Bronx, New York 10461*

Background: Cytosolic carboxypeptidases (CCPs) are a subfamily of enzymes that modify tubulin.
Results: Zebrafish CCPs exhibit overlapping expression in developing organs. Knockdown of CCP1 and CCP5 results in similar defects including severe hydrocephalus and axial curvature.
Conclusion: Loss of deglutamylating enzymes causes developmental defects in zebrafish.
Significance: CCP1 and CCP5 play important roles in zebrafish embryonic development.

The cytosolic carboxypeptidases (CCPs) are a subfamily of metalloenzymes within the larger M14 family of carboxypeptidases that have been implicated in the post-translational modification of tubulin. It has been suggested that at least four of the six mammalian CCPs function as tubulin deglutamylases. However, it is not yet clear whether these enzymes play redundant or unique roles within the cell. To address this question, genes encoding CCPs were identified in the zebrafish genome. Analysis by quantitative polymerase chain reaction indicated that CCP1, CCP2, CCP5, and CCP6 mRNAs were detectable between 2 h and 8 days postfertilization with highest levels 5–8 days postfertilization. CCP1, CCP2, and CCP5 mRNAs were predominantly expressed in tissues such as the brain, olfactory placodes, and pronephric ducts. Morpholino oligonucleotide-mediated knockdown of CCP1 and CCP5 mRNA resulted in a common phenotype including ventral body curvature and hydrocephalus. Confocal microscopy of morphant zebrafish revealed olfactory placodes with defective morphology as well as pronephric ducts with increased polyglutamylation. These data suggest that CCP1 and CCP5 play important roles in developmental processes, particularly the development and functioning of cilia. The robust and similar defects upon knockdown suggest that each CCP may have a function in microtubule modification and ciliary function and that other CCPs are not able to compensate for the loss of one.

The M14 metallocarboxypeptidase (CP)[4] family contains ~25 distinct members in most mammalian species; these proteins have been divided into subfamilies based on amino acid sequence homology (1). Members of the A/B subfamily include the well studied pancreatic digestive enzymes CPA1, CPA2, and CPB1 as well as other members expressed in non-pancreatic tissues and presumably functioning in the degradation or processing of endogenous proteins and peptides (2). Most members of the A/B subfamily contain an N-terminal "pro" domain that largely comprises β-sheet structures (3). Members of the N/E subfamily of CPs are involved in the biosynthesis of neuropeptides and peptide hormones, growth factors, and extracellular peptides. The N/E subfamily members do not contain an N-terminal prodomain but instead have a β-sheet-rich structure attached to the C terminus of the CP domain (4, 5). All members of the A/B and N/E subfamilies of CPs are either secreted or found within the secretory pathway. In contrast, a third subfamily of CPs has been identified with expression primarily in the cytosol (1, 6). In humans, there are six of these cytosolic carboxypeptidases (CCPs), named CCP1 through CCP6.

The first identified cytosolic carboxypeptidase, CCP1, was initially named Nna1 because it was reported to be neuronal, nuclear, and induced by axotomy (7). Subsequent studies found that murine CCP1 mRNA is expressed at high levels in many non-neuronal tissues (6, 8) and that the majority of CCP1 protein resides in the cytosol (6) and cycles into the nucleus because of the presence of nuclear localization (9) and nuclear export signals (10). CCP1 is encoded by the *Agtpbp1* gene. In 2002, it was reported that the Purkinje cell degeneration (*pcd*) mouse has a mutation in the *Agtpbp1* gene that results in truncation of CCP1 protein and loss of the active carboxypeptidase domain (8, 11). A number of distinct mutations in the mouse *Agtpbp1* gene all cause the death of Purkinje cells as well as other cell types including olfactory bulb mitral cells, retinal photoreceptor cells, and testis spermatocytes. The genes encoding other members of the CCP gene family were named *Agbl1* through *Agbl5* for the human and mouse genes. In zebrafish, most of the gene names are similar to those of the human and mouse with the exception of the gene encoding zebrafish CCP2 (which was named *zte25*). To reduce confusion, the protein names and not the gene names are used in the present report.

* This work was supported, in whole or in part, by National Institutes of Health Grant 1R01DA-004494 (to L. D. F.).
[S] This article contains supplemental Fig. S1.
[1] Both authors contributed equally to this work.
[2] Present address: Dept. of Biology, Andrews University, Berrien Springs, MI 49104.
[3] To whom correspondence should be addressed: Dept. of Molecular Pharmacology, Albert Einstein College of Medicine, 1300 Morris Park Ave., Bronx, NY 10461. Tel.: 718-430-4225; Fax: 718-430-8954; E-mail: lloyd.fricker@einstein.yu.edu.
[4] The abbreviations used are: CP, carboxypeptidase; CCP, cytosolic carboxypeptidase; *pcd*, Purkinje cell degeneration; hpf, hours postfertilization; dpf, days postfertilization; qPCR, quantitative PCR; MO, morpholino oligonucleotide.

The functions of the CCPs are not entirely clear. Recent evidence suggests that some of the CCPs participate in the processing of tubulin (12–15), which undergoes a number of C-terminal and side chain modifications that affect its function (16). For example, α-tubulin is translated with a C-terminal tyrosine that is removed by a carboxypeptidase to produce detyrosinated tubulin (17–19). Tyrosine can be reattached to the C terminus of detyrosinated tubulin by a selective ligase, tubulin-tyrosine ligase (20, 21). Alternatively, the C-terminal glutamate residue of detyrosinated α-tubulin can be removed by a carboxypeptidase to produce Δ2 tubulin (22). Both α- and β-tubulins are also modified by ligases that attach a glutamate residue to the γ-carboxylate side chain of specific glutamate residues located near the C terminus of the protein (23). Other ligases attach additional glutamates to the C-terminal carboxylate group of the side chain, extending the length of the side chain. In addition, other ligases attach glycine residues to the γ-carboxylate side chain and/or extend the glycine side chain.

The glutamates and/or glycines attached to the side chain of α- and β-tubulins are removed by carboxypeptidases. Evidence that CCPs perform various steps in the processing of tubulin has been provided by studies examining the effect of overexpression or knockdown of the CCPs in cell lines. From these analyses, it was suggested that CCP2 removes tyrosine from α-tubulin to generate detyrosinated tubulin (24); CCP1, CCP4, and CCP6 remove glutamate from the C terminus of detyrosinated tubulin to generate Δ2 tubulin and reduce the length of polyglutamate side chains; and CCP5 selectively removes the γ-linked glutamate from the side chain (12). Studies examining the enzymatic activity of purified CCP1 have shown that this enzyme can remove glutamates from the side chains of α- and β-tubulins and from the C terminus of detyrosinated α-tubulin (13). Similar studies performed with purified CCP5 show that this enzyme can rapidly remove the branch point glutamate and more slowly removes C-terminal glutamates from tubulin (25).

In this study, we utilized the zebrafish system to compare the expression, distribution, and biological functions of CCPs. In light of the studies from Berezniuk *et al.* (25) showing the multifunctionality of CCP5 and a clear overlap in function with CCP1, we sought to determine whether this overlap was reflected in the biological functions of these enzymes. Our results suggest that although these enzymes exhibit overlapping enzymatic functions they play unique roles in zebrafish biology. We describe clear differences in the temporal and spatial distributions of these enzymes and demonstrate a role for both CCP1 and CCP5 in embryogenesis. Additionally, we demonstrate differences in detectable levels of tubulin isoforms in whole body protein extracts after knockdown of CCP5 mRNA, suggesting a major role for this enzyme in the processing of zebrafish tubulin.

EXPERIMENTAL PROCEDURES

Zebrafish Care—Zebrafish (*Danio rerio*, AB strain) were maintained within the Zebrafish Facility of the Albert Einstein College of Medicine according to standard conditions as described previously (26) and as stipulated in an approved Institutional Animal Care and Use Committee protocol. Zebrafish embryos were obtained from wild type fish by natural pairwise matings. Embryos were maintained at 28 °C and injected with morpholino oligonucleotides between the one- and two-cell stages (27). Morpholino oligonucleotides were obtained from Gene Tools, LLC (Philomath, OR) and dissolved in distilled water. GeneTools standard control was used. Morpholino oligonucleotide sequences were as follows: CCP1-MO1, GGTGTTCTGTACGAAAACATCAAGT; CCP1-MO2, TTAAGAACACCAAAACTCACCGACA; CCP5-MO, ATGACCTGCACACACAAGATCAACA. In each experiment, 6 ng of morpholino oligonucleotide were used for the morpholinos directed against CCP1 mRNA, and 3 ng were used for those directed against CCP5 mRNA. Control morpholino oligonucleotide was matched for ng amount with experimental morpholino oligonucleotides.

cDNA Synthesis—RNA was extracted from zebrafish embryos using the RNeasy Mini kit (Qiagen) according to the protocol for animal tissues. RNA quality was assessed by formaldehyde gel electrophoresis. First strand cDNA synthesis was performed using the Superscript III First Strand Synthesis System (Invitrogen).

cDNA Cloning—Amplification of desired cDNAs was performed by PCR with PfuUltraII DNA polymerase (Stratagene) using a program of 95 °C for 2 min followed by 40 cycles of 95 °C for 30 s, 58 °C for 30 s, and 72 °C for 2 min. For primer sequences, contact the authors. A 3′ overhang was added to each amplicon by incubating with *Taq* polymerase at 72 °C for 10 min. Cloning into the pCRII-TOPO plasmid (Invitrogen) was performed by TOPO TA cloning according to the manufacturer's instructions. All cloning was verified by sequencing.

Quantitative PCR—Quantitative PCR (qPCR) was performed on an ABI 7900 using Power SYBR® Green PCR Master Mix (Applied Biosystems). Data were normalized to β-actin expression and are shown as relative expression. For primer sequences, contact the authors.

In Situ Hybridization—Probes for *in situ* hybridization were generated by *in vitro* transcription from a linearized plasmid template using a DIG RNA Labeling kit (Roche Applied Science) with T3 or T7 RNA polymerase according to the manufacturer's protocol. Lithium chloride-precipitated RNA probe was redissolved in water, and quality was assessed by formaldehyde gel electrophoresis. Zebrafish embryos were fixed in 4% paraformaldehyde in phosphate-buffered saline (PBS) overnight at 4 °C and processed for *in situ* hybridization according to standard protocols (28) using a probe hybridization temperature of 70 °C. Embryos were finally incubated with the alkaline phosphatase substrate BM purple (Roche Applied Science) in coloration buffer for 8 h at room temperature, reactions were stopped by incubation in 0.1 M glycine, pH 2.2 for 10 min, and embryos were transferred to 70% glycerol for imaging.

Immunostaining and Confocal Microscopy—Zebrafish embryos were collected at 48 hpf, euthanized using an overdose of tricaine, and fixed in 4% paraformaldehyde. Embryos were washed with PBS and transferred to cold 100% acetone at −20 °C for 20 min. Embryos were washed with PBS, bleached in 3% hydrogen peroxide, and incubated in PBS containing 5% bovine serum albumin (BSA). After incubation, medium was removed, and embryos were incubated with PBS containing 0.5% Tween 20 (PBST) containing 5% BSA and antibodies directed against the

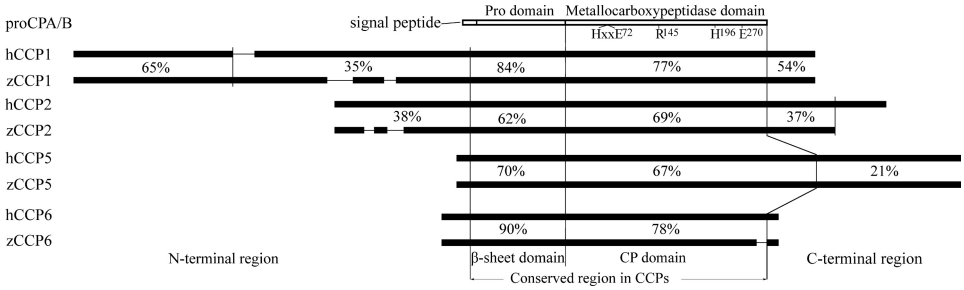

FIGURE 1. **Alignments of CCPs found in humans and zebrafish.** Human and zebrafish protein sequences were retrieved from the National Center for Biotechnology Information database and aligned using ClustalW. CCP sequences (*black bars*) are proportional to length in amino acids. Gaps are indicated where one homolog contains a region that does not correspond to the sequence of the other. All four pairs of homologs contain a β-sheet domain and a metallocarboxypeptidase domain, whereas the N-terminal and C-terminal regions vary between family members and may consist of more than one functional domain. Percent identity is shown between human (*h*) and zebrafish (*z*) homologs. For comparison, a diagram of proCPA1 and proCPB1 is included (*open bar*). Members of the CPA/B subfamily have a prodomain in place of the β-sheet-containing domain of the CCPs. Selected residues required for enzymatic function that are conserved throughout all active enzymes in the metallocarboxypeptidase family are indicated using the numbering system of the mature form of bovine CPA1 by convention.

following epitopes at the indicated dilution: polyglutamylation (1:1500; a gift from Martin A. Gorovsky) and acetylated tubulin (1:600; Sigma-Aldrich, clone 6-11B-1). Embryos were washed in PBST and incubated in PBST containing 5% BSA and 1:400 dilutions of the polyclonal secondary antibodies DyLight 549 anti-mouse and DyLight 488 anti-rabbit. Embryos were washed in PBST and transferred to a mounting medium composed of 53% benzyl alcohol (by weight), 45% glycerol (by weight), and 2% *N*-propyl gallate (29) in glass bottom microwell dishes (MatTek). Images were captured using a Zeiss SP2 confocal microscope. Two-color confocal z-series images were acquired using sequential laser excitation.

Protein Extraction, SDS-PAGE, and Western Blotting—Zebrafish embryos were harvested at 2 dpf, anesthetized using tricaine, dechorionated, and deyolked according to the methods described in Link *et al.* (30). Deyolked embryos were combined with SDS sample buffer and incubated for 15 min at 95 °C. SDS-PAGE was performed according to standard procedures followed by transfer to nitrocellulose paper. Blots were incubated with antibodies against polyglutamylation (1:1500) and α-tubulin (1:5000; clone DM1A, Sigma-Aldrich) followed by HRP-conjugated secondary antibodies (1:2000; Cell Signaling Technology). Band densities were calculated using ImageJ software.

RESULTS

Identification and Comparison of Zebrafish CCPs—The zebrafish nucleotide collection and genomic databases were searched for orthologs of human CCPs. The nucleotide collection, which represents mRNA sequences, contained full-length sequences of zebrafish orthologs of CCP1, CCP2, and CCP5 (Fig. 1 and supplemental Fig. S1). These orthologs were also detected in the zebrafish genomic database. The nucleotide collection contained partial sequences of a zebrafish ortholog of CCP6, and together with searches of the genomic database and the expressed sequence tag database, it was possible to piece together the full-length zebrafish CCP6 (Fig. 1 and supplemental Fig. S1). An ortholog of CCP4 was present in the zebrafish genomic database, but this was not detected in the nucleotide collection representing mRNA sequences or in the expressed sequence tag database, which also represents mRNA sequences. Thus, although the genomic sequences could be spliced together into an appropriate open reading frame for a zebrafish ortholog of CCP4, the absence of any sequences in the mRNA-derived databases suggest that this gene is expressed at extremely low levels, is expressed in a very restricted cell type, or is a pseudogene. Several oligonucleotide primers were designed to amplify a putative zebrafish ortholog of CCP4 from cDNA libraries of 2-dpf zebrafish, but no PCR product was obtained of the expected size even after 40 cycles (data not shown). No ortholog of the gene encoding mammalian CCP3 was detected in the zebrafish genomic or mRNA-derived databases.

Zebrafish CCP1, CCP2, CCP5, and CCP6 are generally similar to their human orthologs in terms of domain structure (Fig. 1 and supplemental Fig. S1). In addition to the CP domain, which has homology to the CP domain of A/B and N/E subfamily enzymes, all CCPs in humans and zebrafish contain a β-sheet-rich domain to the N-terminal side of the CP domain. Although there is no sequence similarity between this domain in the CCPs and the prodomain in the CPA/B subfamily of enzymes, the size of the domain and the high degree of β-sheet secondary structure are similar among the A/B and CCP subfamilies (31). The β-sheet domain in the CCPs is likely to be functional based on the high degree of sequence identity between human and zebrafish orthologs (Fig. 1 and supplemental Fig. S1). For CCP1, CCP5, and CCP6, the degree of sequence identity within the β-sheet domain is greater than within the functional CP domain. In addition to the β-sheet and CP domains, CCP1, CCP2, and CCP5 contain additional N-terminal and/or C-terminal domains. For CCP1, the N-terminal 300 amino acids are well conserved between human and zebrafish (65% amino acid identity), and the C-terminal region also shows reasonably high conservation (54% identity). The nuclear export signal localized to the N-terminal region and the nuclear localization signal in the C-terminal region of human CCP1 (9, 10) are highly conserved in zebrafish CCP1 (supplemental Fig. S1). Other regions of the N-terminal portion of CCP1 as well as the N-terminal and/or C-terminal regions of CCP2 and CCP5 show moderate conservation with 21–38% amino acid identity between human and zebrafish orthologs (Fig. 1). In addition, CCP5 contains a unique insertion within the CP domain that adds ~90 residues to the length of this

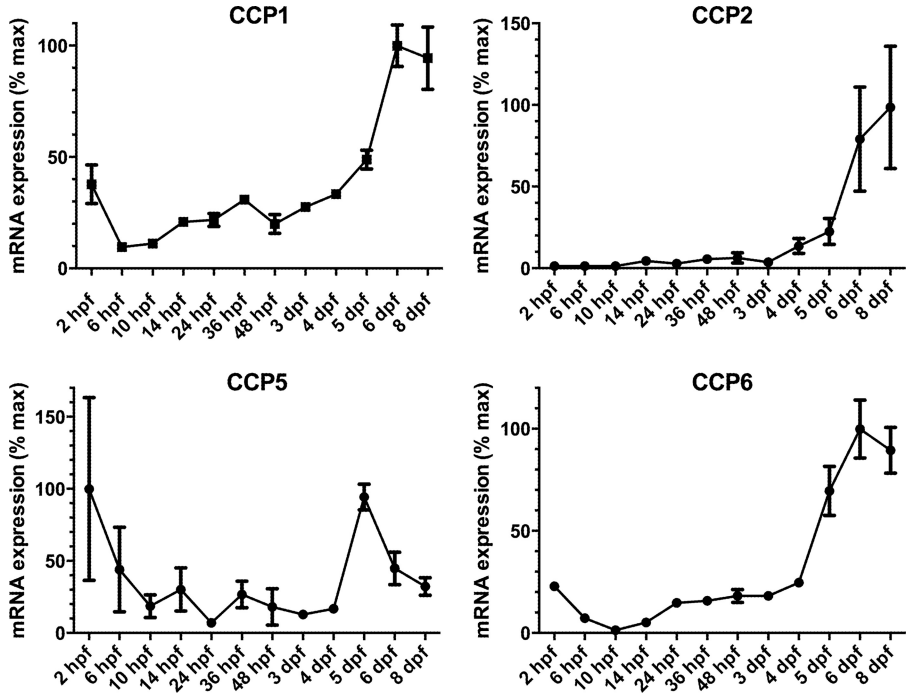

FIGURE 2. **Time course of mRNA expression during the first 8 days of zebrafish development.** Zebrafish were collected at the time points indicated, and levels of mRNA for each of the CCPs were quantified by qPCR. Data points indicate the average level of mRNA transcript, averaged from three independent RNA samples (each a pool of six animals), normalized to β-actin, and plotted as a percentage of the maximum level observed over the time course examined. *Error bars* show S.E.

region; this feature is conserved between human and zebrafish CCP5 orthologs (Fig. 1 and supplemental Fig. S1).

The gene encoding CCP2 is officially named *zte25* (zebrafish testis expressed) because expression in adult zebrafish is restricted to the testis. UniGene reports 19 CCP2 expressed sequence tags, 18 of which are from the testis, and one from olfactory epithelium. Zebrafish CCP1, CCP5, and CCP6 mRNAs have not been reported in the literature other than *in situ* hybridization data deposited to ZFIN for CCP5.[5]

Distribution of Zebrafish CCP mRNAs—The time course of expression for each CCP mRNA during zebrafish development was determined by qPCR analysis. All CCP mRNA data were normalized to β-actin mRNA expression and made relative to maximal expression. The results indicated a small initial drop in CCP1, CCP5, and CCP6 mRNA levels (Fig. 2) likely due to the expression of maternal transcripts at 2 hpf. Levels of CCP1, CCP2, and CCP6 mRNAs gradually increased during development with a large increase at about 6–8 dpf. Levels of CCP5 mRNA were variable at the earliest time points measured and showed an increase at 5 dpf relative to earlier and later time points (Fig. 2).

In situ hybridization was performed to compare the expression patterns of zebrafish CCP1, CCP2, CCP5, and CCP6 mRNA levels at early time points (Fig. 3). At 24 hpf, CCP1 and CCP5 mRNAs were expressed broadly throughout the embryo with concentrated expression in the olfactory placode. By 48 hpf, CCP1 and CCP5 mRNAs were particularly strong within the brain, whereas CCP5 and CCP2 transcripts could be detected within the olfactory placodes as well as the pronephric ducts. Expression of CCP6 mRNA could not be detected by *in situ* hybridization at any time point examined.

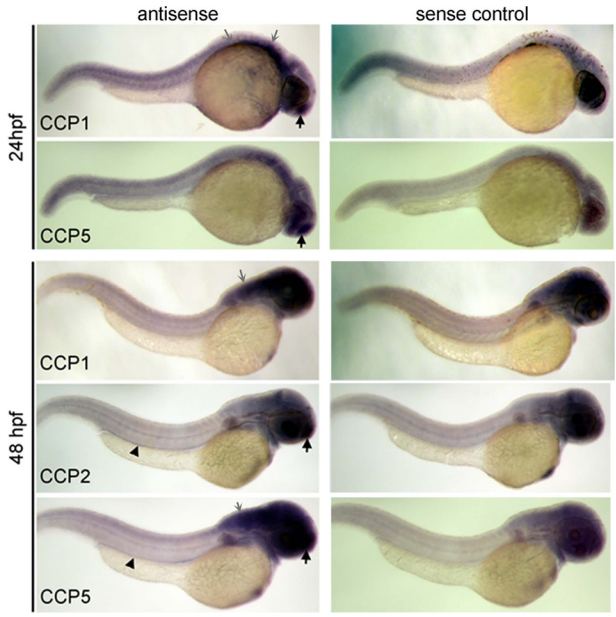

FIGURE 3. ***In situ* hybridization of zebrafish CCP mRNA at 24 and 48 hpf.** Transcripts of CCP1 and CCP5 show strong expression at the olfactory placode (*black arrows*) at 24 hpf, whereas CCP2 and CCP5 show expression in this region at 48 hpf (*black arrows*). Expression of CCP2 and CCP5 mRNA transcripts is observed in the pronephric duct at 48 hpf (*arrowheads*). Expression throughout the brain (*gray arrows*) can be seen for CCP1 at 24 and 48 hpf and for CCP5 at 48 hpf. *In situ* hybridization for each probe and developmental stage was performed on 8–10 embryos; representative results from a single animal are shown.

Functional Analysis of CCP Knockdown—The function of CCP1 and CCP5 was investigated using morpholino antisense

[5] B. Thisse and C. Thisse (2004) Fast release clones: a high throughput expression analysis. ZFIN direct data submission.

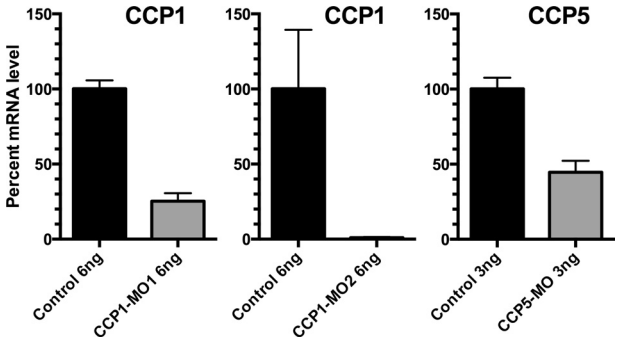

FIGURE 4. **Quantification of mRNA levels of target genes in embryos injected with morpholino oligonucleotides.** Zebrafish embryos were collected at 48 hpf and analyzed by qPCR for CCP mRNA levels. Levels of β-actin mRNA were measured as a control, and the level of CCP mRNA is expressed relative to β-actin. Experiments were performed in triplicate. The entire analysis was performed twice on different groups of animals (each a pool of six animals). *Error bars* show the range of these two separate analyses.

oligonucleotides (Fig. 4). Morpholino oligonucleotides were injected into zebrafish embryos soon after fertilization (one- to two-cell stage) to knock down gene expression during early stages of development by interfering with mRNA splicing. Two splice-blocking morpholino oligonucleotides were designed to interfere with CCP1 mRNA splicing. Injection of 6 ng of CCP1-MO1, which was designed to interfere with splicing between exons 4 and 5, resulted in an 80% decrease in CCP1 mRNA levels at 2 dpf compared with 6 ng of a control morpholino oligonucleotide (Fig. 4, *left panel*). A second morpholino oligonucleotide to CCP1 (CCP1-MO2), designed to interfere with splicing between exons 5 and 6, resulted in a 95% decrease in CCP1 mRNA levels at 2 dpf (Fig. 4, *middle panel*). Injection of 3 ng of a splice-blocking morpholino oligonucleotide to CCP5, designed to interfere with splicing between exons 2 and 3 of the CCP5 gene, resulted in a 55% decrease in the level of CCP5 mRNA at 2 dpf (Fig. 4, *right panel*). Analysis of the morphology of the embryos after morpholino oligonucleotide-mediated knockdown of both CCP1 and CCP5 mRNA showed similar phenotypes: hydrocephalus and body curvature (Fig. 5). These phenotypes were consistently observed in CCP5-MO-injected fish with >75% exhibiting a dramatic axial curvature and greatly enlarged brain ventricles (Fig. 5). Fish injected with CCP1-MOs exhibited greater variability with ~50% of embryos exhibiting normal morphology (Fig. 5). In addition to these brain ventricle and axial curvature phenotypes, both CCP1 and CCP5 morphant zebrafish also displayed a reduction in eye size.

The enlarged ventricles observed in CCP1 and CCP5 morphant zebrafish embryos were examined in greater detail. The two different morpholino oligonucleotides designed to block CCP1 splice sites both increased the size of the ventricles (Fig. 6*A*). Quantification of the area of the ventricle from a two-dimensional side view using the method of Teng *et al.* (33) showed that ventricle area in all CCP1 morphant embryos was 2.5 times that of control MO-injected embryos, representing a large increase in ventricle size (Fig. 6*B*). Embryos injected with CCP5-MO had a comparable increase in ventricle size (Fig. 6*B*). To validate the result with the CCP5 morpholino oligonucleotide, we used a rescue approach with CCP5 mRNA. Injection of 500 pg of CCP5 mRNA did not produce a ventricle size or axial curvature phenotype at 2 dpf (Fig. 6, *A* and *B*), although injection of higher doses of CCP5 mRNA occasionally resulted in a rare severely deformed phenotype (data not shown). The co-injection of 500 pg CCP5 mRNA with 3 ng of CCP5 morpholino oligonucleotide greatly reduced the increase in ventricle size produced by the morpholino oligonucleotide alone (Fig. 6, *A* and *B*), although there was still a small increase compared with control morpholino oligonucleotide-injected embryos (Fig. 6*B*). Analysis of the phenotype of the CCP5 mRNA rescue of CCP5 morphants showed a dramatic decrease in the frequency of embryos displaying hydrocephalus and axial curvature phenotypes compared with the CCP5 morpholino oligonucleotide-injected embryos (Fig. 6*C*).

Based on localization to the developing olfactory placode and previously reported roles for CCP family members in tubulin processing and ciliary function (12, 13, 15, 34), the olfactory placode was examined by confocal microscopy using acetylated tubulin and polyglutamate antibodies to identify the tubulin-rich ciliated cells of the olfactory placode (35, 36). Both the acetylated tubulin and polyglutamate antibodies showed robust immunofluorescent staining of the olfactory placode. In embryos injected with either CCP1-targeted or CCP5-targeted morpholino oligonucleotides, olfactory placode morphology was disrupted, resulting in reduced olfactory placode size and a large increase in polyglutamylated tubulin immunoreactivity in cell bodies relative to cilia (Fig. 7). Confocal microscopy of the cloacal region of the pronephric duct indicated an accumulation of polyglutamylation in the lumen of the duct in a subset of CCP1 morphants (Fig. 7, *M–O*), consistent with a role for CCP1 in deglutamylation. To investigate whether tubulin isoforms were affected by CCP1 and CCP5 knockdown, whole fish lysates were probed with antibodies to detect polyglutamylation. In CCP5 morphant fish, polyglutamylation levels of tubulin relative to total α-tubulin were 2.5 times the levels in controls (Fig. 8), indicating an accumulation of polyglutamylated tubulin isoforms in these animals. Polyglutamylation levels in CCP1 morphants were not different from controls.

DISCUSSION

CCP1 was first identified as a neuronal protein that was induced during axonal regeneration (7). Shortly after this identification, CCP1 was further implicated in neuronal functions when a mutation in the gene encoding CCP1 was found to be responsible for the neuronal degeneration seen in the *pcd* classical mouse mutant (8, 11, 37). Although this discovery was certainly a breakthrough and an answer to a long-standing question, it did not rapidly lead to a clear understanding of the normal function of CCP1. Subsequent discovery of a number of related CCPs (1, 6) led to many more questions. A key question was whether the CCPs function in redundant or complementary pathways. In this report, we have begun to answer this question using the zebrafish model system. The zebrafish system has many advantages including ease of gene expression analysis by *in situ* hybridization and gene expression knockdown by morpholino oligonucleotides. Using these techniques, we have found many similarities in CCP expression and function between the zebrafish system and mammalian organisms such as the mouse.

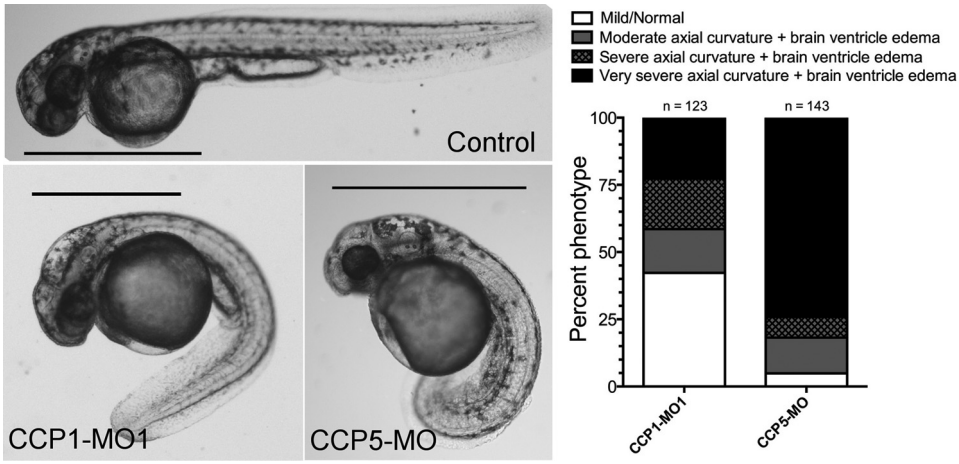

FIGURE 5. **Phenotypes of zebrafish embryos injected with morpholino oligonucleotides targeting CCP1 and CCP5 mRNAs.** Zebrafish embryos were injected with control MO, CCP1-MO1, or CCP5-MO as indicated and collected at 48 hpf for analysis. Embryos injected with CCP1-MO1 or CCP5-MO showed similar phenotypes of severe hydrocephalus (*arrows*) and axial curvature. Embryos injected with CCP5-MO showed more severe phenotypes on average, and a higher percentage of them displayed these phenotypes. *Scale bars* for each image represent 1 mm. Zebrafish were dechorionated and observed at 2 dpf and were classified according to severity of brain ventricle edema and axial curvature. Percentages of fish displaying normal, moderate, severe, and very severe edema and axial curvature are shown (*right*). For CCP1, a total of 123 animals was analyzed; for CCP5, a total of 143 animals was analyzed.

Most previous work on the CCPs has been done using mice in large part because of the existence of the *pcd* mouse mutant and its well characterized phenotype including degeneration of Purkinje cells, olfactory neurons, and photoreceptors (9). Although it is difficult to directly compare the mouse and the zebrafish, there are some similarities to be noted in the perturbation of CCP1 expression in both of these systems. In both the mouse and the zebrafish, CCP1 orthologs are highly expressed across a range of cells and tissues (6). CCP1 mRNA is most highly expressed in the zebrafish brain, consistent with expression patterns of CCP1 mRNA in the mouse and with the neuronal phenotypes of the *pcd* mutants (11). Our study indicated a smaller eye size in CCP1 and CCP5 morphants that could be related to photoreceptor degeneration, although this does not normally occur in the *pcd* mouse until relatively late in development (38, 39). Finally, the broad expression of CCP1 mRNA at early developmental stages but viability of morphant embryos suggests partial redundancy of function. This is supported by the high level of knockdown of CCP1 mRNA by morpholino oligonucleotides but incomplete penetrance of the resulting phenotype. These results are also consistent with the finding that CCP5 and CCP1 have partially overlapping enzyme activities as shown by Berezniuk *et al.* (25).

In contrast to CCP1 mRNA, CCP2 mRNA was not detected at 24 hpf, and when it was detected at 48 hpf, it was only seen in the pronephric ducts and the olfactory placodes. Analysis by qPCR indicated very low levels of expression until a dramatic increase around 5 dpf. This limited expression is consistent with the name of the gene encoding zebrafish CCP2, *zte25*, given because adult expression is enriched in the testes (40). In the mouse, CCP2 is also highly expressed in the testes and poorly expressed in other tissues (6). It may be that CCP2 plays a more important role in the adult. Recently, it has been shown in HeLa cells that CCP2 colocalizes with γ-tubulin within centrioles and with polyglutamylated tubulin within the basal bodies of primary cilia (34). One study suggested that CCP2 functions as a tubulin tyrosine carboxypeptidase (24). However, if this is the case, one would expect a broader distribution for CCP2; detyrosinated tubulin is found in stable microtubules within many types of differentiated cells (41), whereas CCP2 mRNA has a restricted distribution in mouse brain and other tissues (6).

A gene encoding a CCP3 ortholog was not identified in the zebrafish nor was any expression of the CCP4 gene detected. A phylogenetic analysis of all cytosolic carboxypeptidases indicates that CCP3 is very closely related to CCP2 (1, 34), whereas CCP4 groups closely with CCP1 (34). It may be that these enzymes are functionally redundant and unnecessary in the zebrafish. Very little has been published regarding CCP3 and CCP4. Rogowski *et al.* (12) reported that CCP4 was able to shorten polyglutamate chains and produce Δ2 tubulin by removing glutamate, a function very similar to that of CCP1. No up-regulation of CCP4 has been detected to compensate for loss of CCP1 in *pcd* mice (13); however, normal levels of CCP4 may be sufficient for some cell types in the absence of CCP1.

Our observation that the knockdown of zebrafish CCP5 is more consistently severe than that of CCP1 suggests that although the two enzymes may have overlapping functions they are not entirely redundant. Berezniuk *et al.* (25) report that CCP5 is more efficient at cleaving the initial γ-linked glutamate of polyglutamate side chains than cleaving glutamate from longer side chains. In contrast, although CCP1 has been reported to also remove the initial γ-linked glutamate of the side chain (13), it is much more efficient at removing glutamate from longer side chains (25). Another difference between CCP1 and CCP5 is the cellular distribution; both proteins are present in cytosol and nucleus, although CCP5 showed greater nuclear localization in a variety of cell types that were examined (6). These differences presumably explain why knockdown of CCP5 mRNA in the zebrafish results in a very consistent phenotype with >95% of embryos exhibiting hydrocephalus and body curvature, whereas knockdown of CCP1 showed a less consistent phenotype. CCP5 transcripts were detected by qPCR throughout development with *in situ* hybridization indicating

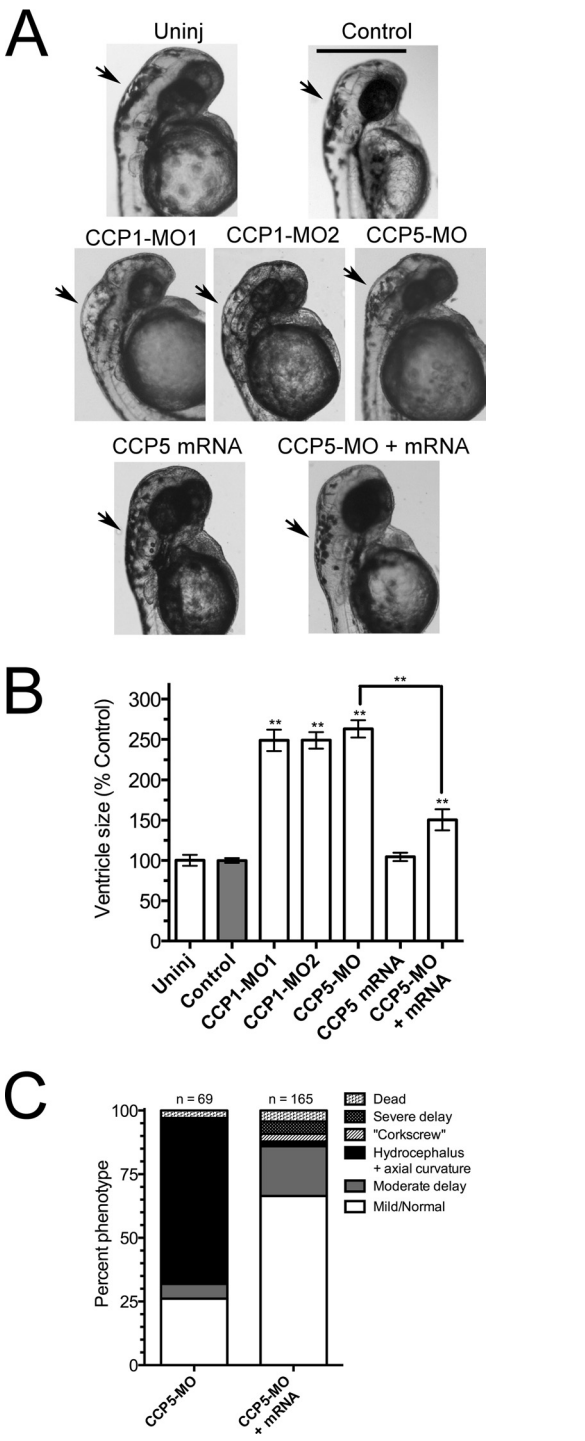

FIGURE 6. **Fish injected with morpholino oligonucleotides against CCP1 and CCP5 show severe hydrocephalus, which can be rescued by co-injection of mRNA.** Zebrafish were collected and visualized at 48 hpf. Hydrocephalus was quantified using ImageJ to calculate the area of a cross-section of the ventricle. *A*, representative images of fish from each group including uninjected fish (*Uninj*) and control morpholino oligonucleotide-injected fish. The *scale bar* indicates 0.5 mm and applies to all images. *Arrows* show brain ventricles. *B*, when quantified, zebrafish embryos injected with 6 ng of CCP1-MOs or 3 ng of CCP5-MO have a brain ventricle with an area ~250% the size of control MO-injected embryos ($p < 0.01$). Embryos injected with 500 pg of mouse CCP5 mRNA have approximately the same size ventricles as control MO-injected embryos. When 500 pg of CCP5 mRNA is co-injected with 3 ng of CCP5-MO, the brain ventricle is smaller than with 3 ng of CCP5-MO alone (**, $p < 0.01$) but larger than control MO-injected embryos (**, $p < 0.01$). Statistics are relative to control MO-injected embryos except where denoted. All statistics were performed using measurements from 10–20 randomly selected embryos per group. *Error bars* show S.E. *C*, CCP5-MO-injected embryos ($n = 69$) and CCP5-MO + mRNA-injected embryos ($n = 165$) were analyzed and classified by phenotype, and the percentage of each phenotype was compared. Embryos co-injected with mRNA show a lower frequency of abnormal phenotypes than embryos injected with CCP5-MO alone.

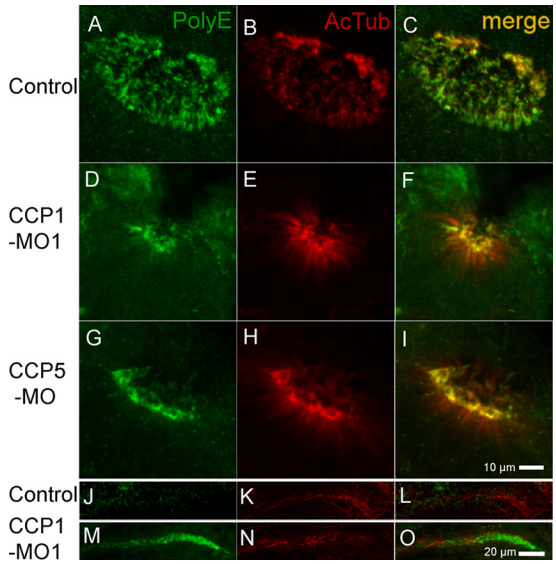

FIGURE 7. **Confocal imaging of ciliated organs in zebrafish embryos.** Zebrafish were collected at 48 hpf and analyzed by immunohistochemistry using acetylated tubulin clone 6-11B-1 (*AcTub*; *red*) and polyglutamate (*PolyE*; *green*) antibodies. Cilia show strong reactivity with both acetylated tubulin clone 6-11B-1 and polyglutamate antibodies in control and morpholino oligonucleotide-injected animals. However, cell bodies, which are not visible in control MO-injected embryos, show reactivity in CCP1-MO1- and CCP5-MO-injected embryos, particularly for the acetylated tubulin clone 6-11B-1 antibody. Additionally, the overall structure of the olfactory placode is altered in morphant embryos, showing tightly clustered cilia and an overall reduction in size. The *scale bar* in *I* applies to *A–I*. At the posterior region of the pronephric duct of severely phenotypic CCP1-MO1-injected animals, there is a large body that shows strong reactivity with the polyglutamate antibody near the cloaca (*M–O*). This reactivity is absent from control animals (*J–L*). The *scale bar* in *O* applies to *J–O*. Staining was performed on at least three groups of >50 embryos each, and representative images are shown.

enrichment in the brain, olfactory placodes, and pronephric ducts and pointing to its necessity in developmental processes. A similar distribution for zebrafish CCP5 mRNA was reported previously in the UniGene database and in ZFIN with expression within Kupffer vesicle during gastrulation also reported.[5] It is notable that injection of CCP5 mRNA occasionally led to a severe curvature phenotype and differences in size and morphology between left and right eyes, potentially indicating a laterality defect controlled by the Kupffer vesicle, which is a ciliated organ.

The accumulation of polyglutamylated tubulin isoforms in CCP5 but not CCP1 morphant embryos indicates that CCP5 disruption leads to widespread changes in the levels of polyglutamylated isoforms of tubulin in developing zebrafish (Fig. 8). It is unclear why CCP1 knockdown would not also show this change but could possibly be explained by compensatory regulation of the enzymes that attach glutamate to tubulin, thereby opposing the actions of CCPs.

Expression of CCP6 mRNA was not detected by *in situ* hybridization in our study. However, it was detected by qPCR through much of zebrafish development. Similar to CCP1 and CCP4, CCP6 has been shown to cleave long polyglutamate

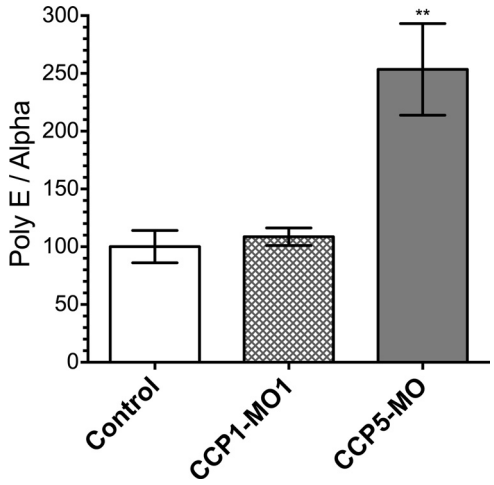

FIGURE 8. **Western blot for polyglutamylated tubulin in whole fish lysate.** Zebrafish were collected at 2 dpf and lysates were analyzed by Western blotting. Membranes were probed with antibodies against α-tubulin (*Alpha*) and polyglutamylated chains (*PolyE*), which at 55 kDa detects primarily polyglutamylated chains on tubulin molecules. Embryos injected with CCP5-MO showed ~2.5-fold reactivity for polyglutamylated tubulin when normalized to α-tubulin, indicating a large increase in tubulin molecules with a polyglutamylated chain (**, $p < 0.01$ compared with control). Zebrafish injected with CCP1-MO did not show a change in polyglutamylation reactivity. *Error bars* show S.E. for four replicates, each replicate consisting of 15–20 animals.

chains (12). CCP6 is one of only two CCPs with an ortholog in *Caenorhabditis elegans*. The *C. elegans* CCP1 ortholog, CCPP-1, plays a role in the localization of kinesin motor proteins through the deglutamylation of tubulin (15). Loss of function of CCPP-1 resulted in an increase in polyglutamylation in specific cilia and defective B-tubules of the ciliary axoneme. A similar function was shown for the *C. elegans* CCP6 ortholog, CCPP-6, although Kimura *et al.* (14) proposed that the *C. elegans* CCPP-6 is a functional CCP5 ortholog. They showed that loss of CCPP-6 gene function resulted in increased polyglutamylation, whereas overexpression resulted in decreased polyglutamylation. In cultured HeLa cells, CCP6 has been found to colocalize with centrioles and basal bodies (34).

The phenotypes seen upon knockdown of either CCP1 or CCP5 mRNA in the zebrafish are consistent with the localization of these genes and are likely due to defective cilium function. Body curvature and enlargement of the brain ventricles have been seen in many morphant zebrafish relevant to cilium function. Knockdown of zebrafish *dyx1c1* resulted in abnormal cilia as well as a prominent body curvature and hydrocephalus (42). Morpholino oligonucleotide-mediated knockdown of the zebrafish ortholog of *DNAAF3*, a gene necessary for the assembly of dynein and its transport into the cilia, disrupted ciliary motility and resulted in hydrocephalus and body curvature among other phenotypes (43). Knockdown of the zebrafish ortholog of nephrocystin-3, mutations of which are responsible for human nephronophthisis type 3 and which localizes to cilia, also resulted in hydrocephalus and body curvature in addition to the expected pronephric cysts (44). A thorough study of the role of cilia and their malfunction leading to hydrocephalus and pronephric cysts has been performed (45). This study indicated that motile cilia were actively involved in creating fluid flow within the pronephros and the central canal of the spinal cord. Without this flow of fluid, whether due to defective cilia or to a mechanical blockage, fluid buildup occurred that led to hydrocephalus and kidney cysts. It is notable that many of these morphants and many mutants that develop pronephric cysts (32) also exhibit ventral body curvature. The reason for this ventral curvature is not clear at this time.

Altogether, our study points to an important developmental function for the CCP proteins. This work and work of others point to a prominent role for the CCPs in the function of cilia, both motile and non-motile, within organs such as the kidneys and the nervous system. Some redundancy of function appears to be built into the system, particularly in the shortening of polyglutamate side chains: four of six mammalian CCPs have now been shown to perform this function. However, many factors point to a specialized role for CCP5 in the efficient removal of the branch point glutamate that initiates these polyglutamate side chains.

Acknowledgments—We thank Christina Polumbo at the Analytical Imaging Facility at Albert Einstein College of Medicine for assistance with confocal imaging and analysis. We give special thanks to Dr. Florence Marlow and members of her research group for advice and assistance with the zebrafish. We also thank Martin A. Gorovsky for the generous gift of the polyglutamate antibody.

REFERENCES

1. Rodriguez de la Vega, M., Sevilla, R. G., Hermoso, A., Lorenzo, J., Tanco, S., Diez, A., Fricker, L. D., Bautista, J. M., and Avilés, F. X. (2007) Nna1-like proteins are active metallocarboxypeptidases of a new and diverse M14 subfamily. *FASEB J.* **21,** 851–865
2. Wei, S., Segura, S., Vendrell, J., Aviles, F. X., Lanoue, E., Day, R., Feng, Y., and Fricker, L. D. (2002) Identification and characterization of three members of the human metallocarboxypeptidase gene family. *J. Biol. Chem.* **277,** 14954–14964
3. Ventura, S., Gomis-Rüth, F. X., Puigserver, A., Avilés, F. X., and Vendrell, J. (1997) Pancreatic procarboxypeptidases: oligomeric structures and activation processes revisited. *Biol. Chem.* **378,** 161–165
4. Gomis-Rüth, F. X., Companys, V., Qian, Y., Fricker, L. D., Vendrell, J., Avilés, F. X., and Coll, M. (1999) Crystal structure of avian carboxypeptidase D domain II: a prototype for the regulatory metallocarboxypeptidase subfamily. *EMBO J.* **18,** 5817–5826
5. Gomis-Rüth, F. X. (2008) Structure and mechanism of metallocarboxypeptidases. *Crit. Rev. Biochem. Mol. Biol.* **43,** 319–345
6. Kalinina, E., Biswas, R., Berezniuk, I., Hermoso, A., Aviles, F. X., and Fricker, L. D. (2007) A novel subfamily of mouse cytosolic carboxypeptidases. *FASEB J.* **21,** 836–850
7. Harris, A., Morgan, J. I., Pecot, M., Soumare, A., Osborne, A., and Soares, H. D. (2000) Regenerating motor neurons express Nna1, a novel ATP/GTP-binding protein related to zinc carboxypeptidases. *Mol. Cell. Neurosci.* **16,** 578–596
8. Fernandez-Gonzalez, A., La Spada, A. R., Treadaway, J., Higdon, J. C., Harris, B. S., Sidman, R. L., Morgan, J. I., and Zuo, J. (2002) Purkinje cell degeneration (pcd) phenotypes caused by mutations in the axotomy-induced gene, Nna1. *Science* **295,** 1904–1906
9. Wang, T., and Morgan, J. I. (2007) The Purkinje cell degeneration (pcd) mouse: an unexpected molecular link between neuronal degeneration and regeneration. *Brain Res.* **1140,** 26–40
10. Thakar, K., Karaca, S., Port, S. A., Urlaub, H., and Kehlenbach, R. H. (2013) Identification of CRM1-dependent nuclear export cargos using quantitative mass spectrometry. *Mol. Cell. Proteomics* **12,** 664–678
11. Mullen, R. J., Eicher, E. M., and Sidman, R. L. (1976) Purkinje cell degeneration, a new neurological mutation in the mouse. *Proc. Natl. Acad. Sci. U.S.A.* **73,** 208–212
12. Rogowski, K., van Dijk, J., Magiera, M. M., Bosc, C., Deloulme, J. C.,

Bosson, A., Peris, L., Gold, N. D., Lacroix, B., Bosch Grau, M., Bec, N., Larroque, C., Desagher, S., Holzer, M., Andrieux, A., Moutin, M. J., and Janke, C. (2010) A family of protein-deglutamylating enzymes associated with neurodegeneration. *Cell* **143,** 564–578

13. Berezniuk, I., Vu, H. T., Lyons, P. J., Sironi, J. J., Xiao, H., Burd, B., Setou, M., Angeletti, R. H., Ikegami, K., and Fricker, L. D. (2012) Cytosolic carboxypeptidase 1 is involved in processing α- and β-tubulin. *J. Biol. Chem.* **287,** 6503–6517
14. Kimura, Y., Kurabe, N., Ikegami, K., Tsutsumi, K., Konishi, Y., Kaplan, O. I., Kunitomo, H., Iino, Y., Blacque, O. E., and Setou, M. (2010) Identification of tubulin deglutamylase among *Caenorhabditis elegans* and mammalian cytosolic carboxypeptidases (CCPs). *J. Biol. Chem.* **285,** 22936–22941
15. O'Hagan, R., Piasecki, B. P., Silva, M., Phirke, P., Nguyen, K. C., Hall, D. H., Swoboda, P., and Barr, M. M. (2011) The tubulin deglutamylase CCPP-1 regulates the function and stability of sensory cilia in *C. elegans*. *Curr. Biol.* **21,** 1685–1694
16. Fukushima, N., Furuta, D., Hidaka, Y., Moriyama, R., and Tsujiuchi, T. (2009) Post-translational modifications of tubulin in the nervous system. *J. Neurochem.* **109,** 683–693
17. Hallak, M. E., Rodriguez, J. A., Barra, H. S., and Caputto, R. (1977) Release of tyrosine from tyrosinated tubulin. Some common factors that affect this process and the assembly of tubulin. *FEBS Lett.* **73,** 147–150
18. Argaraña, C. E., Barra, H. S., and Caputto, R. (1978) Release of [^{14}C]tyrosine from tubulinyl-[^{14}C]tyrosine by brain extract. Separation of a carboxypeptidase from tubulin-tyrosine ligase. *Mol. Cell. Biochem.* **19,** 17–21
19. Argarana, C. E., Barra, H. S., and Caputto, R. (1980) Tubulinyl-tyrosine carboxypeptidase from chicken brain: properties and partial purification. *J. Neurochem.* **34,** 114–118
20. Arce, C. A., Rodriguez, J. A., Barra, H. S., and Caputo, R. (1975) Incorporation of L-tyrosine, L-phenylalanine and L-3,4-dihydroxyphenylalanine as single units into rat brain tubulin. *Eur J. Biochem.* **59,** 145–149
21. Barra, H. S., Arcce, C. A., Rodriguez, J. A., and Caputto, R. (1973) Uncorporation of phenylalanine as a single unit into rat brain protein: reciprocal inhibition by phenylalanine and tyrosine of their respective incorporations. *J. Neurochem.* **21,** 1241–1251
22. Paturle-Lafanechère, L., Manier, M., Trigault, N., Pirollet, F., Mazarguil, H., and Job, D. (1994) Accumulation of Δ2-tubulin, a major tubulin variant that cannot be tyrosinated, in neuronal tissues and in stable microtubule assemblies. *J. Cell Sci.* **107,** 1529–1543
23. Eddé, B., Rossier, J., Le Caer, J. P., Desbruyères, E., Gros, F., and Denoulet, P. (1990) Posttranslational glutamylation of α-tubulin. *Science* **247,** 83–85
24. Sahab, Z. J., Hall, M. D., Me Sung, Y., Dakshanamurthy, S., Ji, Y., Kumar, D., and Byers, S. W. (2011) Tumor suppressor RARRES1 interacts with cytoplasmic carboxypeptidase AGBL2 to regulate the α-tubulin tyrosination cycle. *Cancer Res.* **71,** 1219–1228
25. Berezniuk, I., Lyons, P. J., Sironi, J. J., Xiao, H., Setou, M., Angeletti, R. H., Ikegami, K., and Fricker, L. D. (2013) Cytosolic carboxypeptidase 5 removes α- and γ-linked glutamates from tubulin. *J. Biol. Chem.* **288,** 30445–30453
26. Kimmel, C. B., Ballard, W. W., Kimmel, S. R., Ullmann, B., and Schilling, T. F. (1995) Stages of embryonic development of the zebrafish. *Dev. Dyn.* **203,** 253–310
27. Westerfield, M. (2007) *The Zebrafish Book. A Guide for the Laboratory Use of Zebrafish (Danio rerio)*, 5th Ed., University of Oregon Press, Eugene, OR
28. Thisse, C., and Thisse, B. (2008) High-resolution *in situ* hybridization to whole-mount zebrafish embryos. *Nat. Protoc.* **3,** 59–69
29. Drummond, I. (2009) Studying cilia in zebrafish. *Methods Cell Biol.* **93,** 197–217
30. Link, V., Shevchenko, A., and Heisenberg, C. P. (2006) Proteomics of early zebrafish embryos. *BMC Dev. Biol.* **6,** 1
31. Otero, A., Rodríguez de la Vega, M., Tanco, S., Lorenzo, J., Avilés, F. X., and Reverter, D. (2012) The novel structure of a cytosolic M14 metallocarboxypeptidase (CCP) from *Pseudomonas aeruginosa*: a model for mammalian CCPs. *FASEB J.* **26,** 3754–3764
32. Drummond, I. A., Majumdar, A., Hentschel, H., Elger, M., Solnica-Krezel, L., Schier, A. F., Neuhauss, S. C., Stemple, D. L., Zwartkruis, F., Rangini, Z., Driever, W., and Fishman, M. C. (1998) Early development of the zebrafish pronephros and analysis of mutations affecting pronephric function. *Development* **125,** 4655–4667
33. Teng, Y., Xie, X., Walker, S., Saxena, M., Kozlowski, D. J., Mumm, J. S., and Cowell, J. K. (2011) Loss of zebrafish lgi1b leads to hydrocephalus and sensitization to pentylenetetrazol induced seizure-like behavior. *PLoS One* **6,** e24596
34. Rodríguez de la Vega Otazo, M., Lorenzo, J., Tort, O., Avilés, F. X., and Bautista, J. M. (2013) Functional segregation and emerging role of cilia-related cytosolic carboxypeptidases (CCPs). *FASEB J.* **27,** 424–431
35. Wloga, D., Webster, D. M., Rogowski, K., Bré, M. H., Levilliers, N., Jerka-Dziadosz, M., Janke, C., Dougan, S. T., and Gaertig, J. (2009) TTLL3 is a tubulin glycine ligase that regulates the assembly of cilia. *Dev. Cell* **16,** 867–876
36. Pathak, N., Obara, T., Mangos, S., Liu, Y., and Drummond, I. A. (2007) The zebrafish fleer gene encodes an essential regulator of cilia tubulin polyglutamylation. *Mol. Biol. Cell* **18,** 4353–4364
37. Chakrabarti, L., Eng, J., Martinez, R. A., Jackson, S., Huang, J., Possin, D. E., Sopher, B. L., and La Spada, A. R. (2008) The zinc-binding domain of Nna1 is required to prevent retinal photoreceptor loss and cerebellar ataxia in Purkinje cell degeneration (pcd) mice. *Vision Res.* **48,** 1999–2005
38. Blanks, J. C., Mullen, R. J., and LaVail, M. M. (1982) Retinal degeneration in the pcd cerebellar mutant mouse. II. Electron microscopic analysis. *J. Comp. Neurol.* **212,** 231–246
39. LaVail, M. M., Blanks, J. C., and Mullen, R. J. (1982) Retinal degeneration in the pcd cerebellar mutant mouse. I. Light microscopic and autoradiographic analysis. *J. Comp. Neurol.* **212,** 217–230
40. Sreenivasan, R., Cai, M., Bartfai, R., Wang, X., Christoffels, A., and Orban, L. (2008) Transcriptomic analyses reveal novel genes with sexually dimorphic expression in the zebrafish gonad and brain. *PLoS One* **3,** e1791
41. Gundersen, G. G., and Bulinski, J. C. (1986) Microtubule arrays in differentiated cells contain elevated levels of a post-translationally modified form of tubulin. *Eur. J. Cell Biol.* **42,** 288–294
42. Chandrasekar, G., Vesterlund, L., Hultenby, K., Tapia-Páez, I., and Kere, J. (2013) The zebrafish orthologue of the dyslexia candidate gene DYX1C1 is essential for cilia growth and function. *PLoS One* **8,** e63123
43. Mitchison, H. M., Schmidts, M., Loges, N. T., Freshour, J., Dritsoula, A., Hirst, R. A., O'Callaghan, C., Blau, H., Al Dabbagh, M., Olbrich, H., Beales, P. L., Yagi, T., Mussaffi, H., Chung, E. M., Omran, H., and Mitchell, D. R. (2012) Mutations in axonemal dynein assembly factor DNAAF3 cause primary ciliary dyskinesia. *Nat. Genet.* **44,** 381–389, S1–S2
44. Zhou, W., Dai, J., Attanasio, M., and Hildebrandt, F. (2010) Nephrocystin-3 is required for ciliary function in zebrafish embryos. *Am. J. Physiol. Renal Physiol.* **299,** F55–F62
45. Kramer-Zucker, A. G., Olale, F., Haycraft, C. J., Yoder, B. K., Schier, A. F., and Drummond, I. A. (2005) Cilia-driven fluid flow in the zebrafish pronephros, brain and Kupffer's vesicle is required for normal organogenesis. *Development* **132,** 1907–1921

Enzymology:

Zebrafish Cytosolic Carboxypeptidases 1 and 5 Are Essential for Embryonic Development

Peter J. Lyons, Matthew R. Sapio and Lloyd D. Fricker

J. Biol. Chem. 2013, 288:30454-30462.
doi: 10.1074/jbc.M113.497933 originally published online September 10, 2013